Anharmonic Vibrational Spectra of Acetylacetone

I. MATANOVIĆ, N. DOŠLIĆ

Department of Physical Chemistry, R. Bošković Institute, Bijenička 54, 10000 Zagreb, Croatia

Received 22 November 2004; accepted 16 February 2005
Published online 12 December 2005 in Wiley InterScience (www.interscience.wiley.com).
DOI 10.1002/qua.20894

ABSTRACT: The spectroscopic proprieties of two energetically close conformers of acetylacetone have been investigated using density functional methods. The calculated anharmonic frequencies are in very satisfactory agreement with experimental data. The low height of the conversion barrier explains why the signature of both conformers can be found in the vibrational spectrum. © 2005 Wiley Periodicals, Inc. Int J Quantum Chem 106: 1367–1374, 2006

Key words: density functional computation; harmonic approximation; anharmonic corrections; infrared spectrum; intramolecular proton transfer

1. Introduction

Studies of the enol form of β-diketones can provide an understanding of the structure and dynamics of intramolecular hydrogen bonds [1, 2]. As the smallest molecules exhibiting intramolecular H-bonding, they provide a solid foundation for the study of H-bonding in complex systems.

The intramolecular H-bond of β-diketones is characterized by highly complex vibrational dynamics: proton transfer (PT) motion along the double minimum potential, coupling of different normal modes, and Fermi resonance [3–6]. Consequently, the (IR) spectra show a broad, red-shifted OH-stretch absorption band. The structure of the bend encodes information on the pathways and time scales of the vibrational energy redistribution processes. Experimental observation of the OH-stretching dynamics, however, became possible only recently with the development of intense femtosecond lasers in the IR domain [7, 8]. Turning to malonaldehyde (MA), the proton transfer model system par excellence, information on the OH-stretching motion is hardly accessible due to the very low intensity of the mode [9, 10]. In contrast, the IR spectrum of acetylacetone (ACAC) is dominated by a strongly broadened OH-stretch band [11–13]. The band is located at 2000–3400 cm^{-1}, with a maximum at $\approx$2800 cm^{-1}. Upon deuteration of the bridging proton, the band center shifts to 2030 cm^{-1}, and the bandwidth is reduced to $\approx$200 cm^{-1}. Using mixed quantum classical density matrix evolution theory, Mavri and Grdadolnik [13, 14] could explain the bulk of these

Correspondence to: N. Došlić; e-mail: nadja.doslic@irb.hr
Contract grant sponsor: Croatian Ministry of Science and Technology.
Contract grant number: 0098033.
Contract grant sponsor: Humboldt Foundation.

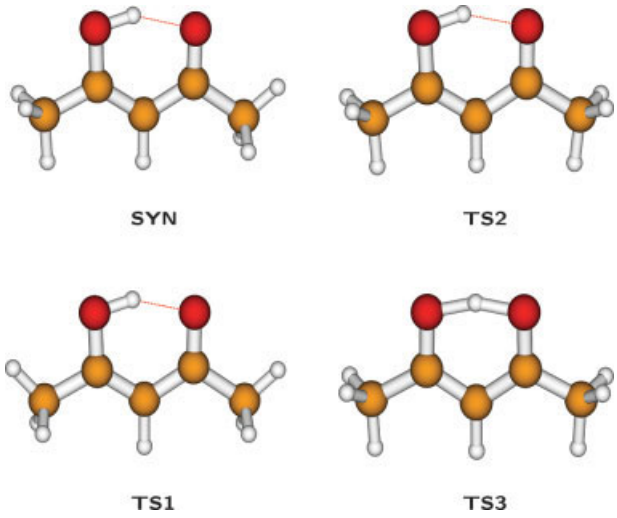

FIGURE 1. Relevant ACAC structures. Top: Global minimum structure (**SYN**), and transition state for rotation of the distal methyl group (**TS2**). Bottom: Transition states for rotation of the proximal methyl group (**TS1**) and for the PT reaction (**TS3**).

effects. Because of the simplified two-state empirical valence form of the potential, however, they could not provide any insight into the mode coupling dynamics.

Currently, the most accurate ab initio vibrational frequency calculation has been reported by Tayyary and Milani-nejad [15], who provide a comprehensive overview of experimental results. Besides the notorious anharmonicity of the OH-stretch band, the vibrational spectrum of ACAC displays intriguing features in the bending modes of the hydrogen bond. A broad, intense line that splits at low temperature into three components is observed at $\approx 1630\,\mathrm{cm}^{-1}$ [16]. The structure of the line has been explained by the presence of two rapidly interconverting forms of the enolic ACAC [15, 16]. Still, in our opinion, a conclusive assignment is missing, since the discrepancies between the harmonic and the observed frequencies are close to $90\,\mathrm{cm}^{-1}$. In the present study, we calculate the anharmonic vibrational spectrum of two, energetically close, conformers of ACAC. By going beyond the harmonic approximation, we will be able not only to improve the agreement with the experiment, but also to understand the nature of the vibrational modes coupling that lead to anharmonicities in the ACAC spectrum.

This study is organized as follows. The computational methods are briefly described in Section 2. In Section 3, the most important stationary points of the enolic ACAC are analyzed first, and then the results of the anharmonic frequency calculations are presented. The study is summarized in Section 4.

2. Computational Methods

Second-order Møller–Plesset perturbation theory (MP2) and density functional theory (DFT) with the B1LYP [17] exchange-correlation functional have been used to optimize the geometries of the stationary points of interest and to determine the relative energies of the these points. All calculations were performed using the Gaussian 03 [18] and Gamess [19] quantum chemical software packages. Harmonic vibrational analysis have been performed to characterize each point as a minimum, a transition state, or a higher-order saddle point. The anharmonic frequencies have been calculated by the second-order perturbative treatment used by Barone and Manichino [20, 21]. The method is implemented in the Gaussian 03 suite of programs [18].

3. Results and Discussion

3.1. ANALYSIS OF THE STATIONARY POINTS

In the gas phase, the energetically preferred structure of ACAC is the *syn*-enol isomer with C_s point-group symmetry (**SYN**)[22–24]. Structures **TS1**, **TS2**, and **TS3**, shown in Figure 1, are first-order transition structures for the two internal rotations of the methyl groups, and for the intramolecular PT reaction between two equivalent *syn*-enol isomers, respectively. Since the geometric and energetic properties of the these stationary points have been investigated in Ref. [24], we summarize the most salient results. The **TS1** structure is 1.45 (1.32) kcal mol^{-1} above the minimum energy structure at the MP2(FC)/6-311G(*d*,*p*) [B1LYP/6-311G(*d*,*p*)] level of theory, while **TS2** is only 0.25 (0.13) kcal mol^{-1} above **SYN** at MP2(FC)/6-311G(*d*,*p*) [B1LYP/6-311G(*d*,*p*)]. The

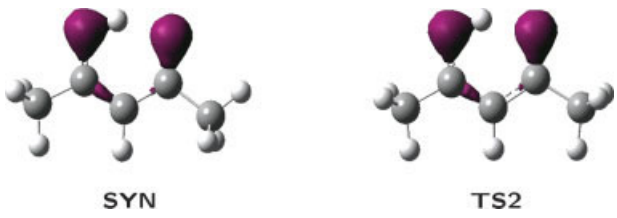

FIGURE 2. Electron density distributions in **SYN** and **TS2** conformers of ACAC at an isosurface value of 0.3 e Å^{-3}.

TABLE I

Vibrational frequencies in cm^{-1} of SYN-ACAC conformer at MP2/6-311G(*d,p*) and B1LYP/6-311G(*d,p*) levels of theory.*

	Exp(s)	Int.	MP2(h)	B1LYP(h)	Int.	B1LYP(a)	Mode
1	—	—	3258	3217	2	3101	ν $CH_{olefinic}$
2	2800	br	3192	3160	85	2766	ν OH
3	3017	10	3206	3151	2	2991	ν_a CH_3
4	3017	10	3202	3144	19	2935	ν_a CH_3
5	2976	6	3166	3101	3	2961	ν_a CH_3
6	2976	6	3164	3098	3	2988	ν_a CH_3
7	2941	7	3085	3048	2	2944	ν_s CH_3
8	2941	7	3080	3043	1	2952	ν_s CH_3
9	1642	19	1716	1700	96	1650	ν_a C═C─C═O + δ OH
10	1624	77	1687	1660	100	1625	ν C═O + δ OH
11	1464	10	1512	1501	14	1464	δ_a CH_3
12	—	—	1494	1485	2	1471	δ_a CH_3
13	—	—	1491	1480	3	1460	δ_a CH_3
14	—	—	1488	1479	3	1438	δ_a CH_3
15	1427	17	1478	1468	47	1443	ν_a CC═CO + δ CH + δ OH + ν C─CH_3
16	—	—	1416	1424	11	1380	δ_s CH_3 + δOH
17	—	—	1443	1402	29	1345	δ OH + ν C═O + ν_s C─C═C─O
18	1365	10	1397	1394	11	1369	δ_s CH_3 + δ OH
19	1250	17	1292	1275	46	1243	ν_s C─C═C + δ OH + ν C─CH_3
20	1171	6	1198	1199	5	1183	δ $CH_{olefinic}$
21	—	—	1069	1072	1	1048	π CH_3
22	—	—	1048	1052	3	1043	π CH_3
23	1025	1	1043	1041	3	1023	ρ CH_3
24	1000	4	1018	1013	4	1017	ρ CH_3
25	952	10	962	968	25	954	γ OH
26	—	—	951	947	1	937	δ C─C═C + ν C─C + ρ CH_3
27	913	9	929	921	11	922	ν C─CH_3 + ν C─O
28	768	40	777	799	11	766	γ $CH_{olefinic}$
29	—	—	627	653	—	653	Γ_{ring}
30	636	9	655	650	4	634	Δ_{ring}
31	—	—	537	556	—	566	Γ_{ring}
32	508	20	509	512	4	513	Δ_{ring}
33	397	s	393	398	1	412	Δ_{ring}
34	362	s	365	371	2	368	ν O···O
35	210	w	225	230	1	238	Γ_{ring} + γ C─CH_3
36	—	—	183	182	—	177	Γ_{ring} + τ CH_3
37	—	—	150	154	—	152	τ CH_3
38	120	w	113	121	1	125	τ CH_3
39	—	—	51	23	—	Not converged	τ CH_3

*Exp. data taken from Ref. [15].
s, gas; h, harmonic; a, anharmonic.

energy of the H-bond, i.e., the energy difference between the *anti* and *syn*-enol forms is 15.4 kcal mol^{-1} at MP2(FC)/6-311G(*d,p*) level of theory.

A very interesting aspect of the PT reaction in ACAC is the coupling of two large-amplitude motions: the rotation of the distal methyl group and the double well motion of the bridging H-atom [25]. Inspection of Figure 1 indeed reveals a different orientation of the methyl groups at a minimum and at the transition state. The calculation of the reaction path for the PT reaction given in Ref. [24] does not support a hypothesis of concerted motion. Instead, our analysis suggests that the PT reaction is triggered only after the methyl groups reaches an eclipsed conformation. To investigate this issue more thoroughly, in Figure 2 we show a contour plot of the correlated

TABLE II

B1LYP/6-311G(*d,p*) vibrational frequencies in cm^{-1} of d2-ACAC SYN conformer.

	Exp(s)	Int.	B1LYP(h)	Int.	B1LYP(a)	Mode
1	3018	w	3152	3	3015	ν_a CH_3 (in plane)
2	3018		3147	3	3000	ν_a CH_3 (in plane)
3	2970	w	3101	2	2961	ν_a CH_3 (out of plane)
4	2970		3098	3	2988	ν_a CH_3 (out of plane)
5	2940	w	3048	2	2943	ν_s CH_3
6	2940		3043	1	2951	ν_s CH_3
7	2300	w	2378	1	2299	ν $CD_{olefinic}$
8	2027		2306	54	2027	ν OD
9	1633	vs	1689	63	1645	ν_a C═C─C═O
10	1544	vs	1582	100	1531	ν_s C═C─C═O + δ OD
11	1448		1488	21	1447	δ_a CH_3 (in plane)
12	—		1485	2	1472	δ_a CH_3 (out of plane)
13	—		1479	2	1443	δ_a CH_3 (out of plane)
14	1448	s	1474	9	1462	δ_a CH_3 (in plane)
15	1408	br	1433	9	1399	ν_a C─C═C─O
16	1365	s	1411	5	1383	δ_s CH_3
17	1365		1391	13	1372	δ_s CH_3
18	1273	vs	1308	32	1274	ν_s C─C═C─O
19	1082	m	1128	15	1102	δ OD + ν C═C + ρ CH_3
20	—		1071	1	1047	π CH_3
21	1025	m	1052	2	1043	π CH_3
22	1025		1051	10	1038	ρ CH_3 + δ OD
23	—		1013	2	1013	ρ CH_3
24	936	m	949	6	940	ν C─CH_3 + ρ CH_3 + δ $CD_{olefinic}$
25	880	w	893	4	891	ν C─O + δ C─C═C + ρ CH_3
26	—		850	—	843	δ $CD_{olefinic}$
27	707	ms	730	12	724	γ OD
28			654	—	640	Γ_{ring}
29	631	m	644	3	631	Δ_{ring}
30	—		573	5	565	γ $CD_{olefinic}$
31	—		554	—	563	Γ_{ring}
32	498	m	503	3	504	Δ_{ring}
33	397	s	391	1	403	Δ_{ring}
34	362	s	364	2	364	ν O···O
35	220	br	226	1	234	ν O···O + δ C─CH_3
36	—		180	—	175	Γ_{ring}
37	—		153	—	149	Γ_{ring}
38	120	br	119	1	126	τ CH_3
39	—		23	—	Not converged	τ CH_3

electron density in the **SYN** and **TS2** structures [26]. Apparently, the charge density in the O···H···O region has been affected only in a limited extent by the rotation of the methyl group. In contrast, a synchronized mechanism would imply a large displacement of charges in the PT moiety.

3.2. VIBRATIONAL SPECTRA

Table I compiles the harmonic frequencies of ACAC at the MP2/6-311G(*d,p*) and B1LYP/6-311G (*d,p*) levels of theory along with the anharmonic frequencies and observed gas-phase transitions. To facilitate comparison with previous studies, we retain the normal-modes interpretation described in Ref. [15]. On average, the deviation from experiment is 0.96%. Although the agreement between computed anharmonic frequencies and experiment is very good, a number of transitions deserve further discussion.

As expected, the largest anharmonicity is observed for the OH-stretching vibration. The OH-stretch

TABLE III

B1LYP/6-311G(*d*,*p*) vibrational frequencies in cm^{-1} of d6-ACAC SYN conformer.

	Exp(s)	Int.	B1LYP(h)	Int.	B1LYP(a)	Mode
1	3098	—	3217	1	3090	ν $CH_{olefinic}$
2	2761	4	3156	95	2680	ν OH
3	2265	2	2337	2	2260	ν_a CD_3 (in plane)
4	2265	2	2332	2	2250	ν_a CD_3 (in plane)
5	—	—	2294	2	2220	ν_a CD_3 (out of plane)
6	—	—	2292	2	2229	ν_a CD_3 (out of plane)
7	2103	—	2192	1	2108	ν_s CD_3
8	2103	—	2187	—	2182	ν_s CD_3
9	1628	100	1692	100	1645	ν_a C═C─C═O + δ OH
10	1606	100	1654	100	1611	ν C═O + δ OH
11	1446	36	1474	48	1447	ν_a C═C─C═O + δ OH + δ_s CH
12	1294	15	1406	32	1326	ν_s C═C─C═O + δ OH + ν C─O
13	1265	59	1287	56	1260	ν_s C─CD_3 + ν_s C─C═C + δ OH
14	1185	21	1209	14	1194	δ $CH_{olefinic}$
15	1075	2	1107	2	1090	δ $CH_{olefinic}$ + δ_a CD_3
16	1051	—	1086	1	1073	δ_a CD_3
17	1051	—	1071	1	1058	δ_s CD_3
18	—	—	1068	4	1044	δ_a CD_3
19	—	—	1066	2	1047	δ_a CD_3
20	1036	2	1059	2	1050	δ_a CD_3
21	952	3	970	28	953	γ OH
22	931	4	959	1	946	ν C─O + δ C─C═C + δ OH
23	—	—	925	1	911	ρ CD_3
24	914	1	912	1	898	ρ CD_3
25	904	3	889	1	875	ν_a C─CD_3
26	812	5	828	3	817	ρ CD_3
27	803	10	792	9	797	ρ CD_3
28	763	3	793	4	759	γ $CH_{olefinic}$
29	585	5	592	4	586	Δ_{ring}
30	—	—	573	—	574	Γ_{ring} + ρ CD_3
31	492	3	489	—	495	Γ_{ring} + ρ CD_3
32	477	10	480	4	480	Δ_{ring} + ρ CD_3
33	360		361	1	372	Δ_{ring} + ρ CD_3
34	337		350	2	341	ν O···O
35	212		208	1	213	Δ_{ring} + ρ CD_3
36	—		167	—	166	Γ_{ring} + ρ CD_3
37	—		136	—	140	Γ_{ring} + ρ CD_3
38	—		95	—	87	τ CD_3
39	—		17	—	Not converged	τ CD_3

fundamental is at 2766 cm^{-1}, in very good agreement with the experiment. Compared with its harmonic value, the transition is red-shifted by 393 cm^{-1}. Upon deuteration of the bridging H-atom (d2-ACAC, Table II), the ν_{OD} frequencies shift to 2027 cm^{-1}, again in agreement with the experiment, while deuteration of the two methyl groups (d6-ACAC, Table III) yield $\nu_{OH} = 2679\,cm^{-1}$, $\sim 80\,cm^{-1}$ above the center of the experimental band. For the deuterated compounds, the average deviation from the experiment is 0.82% (d2-ACAC) and 0.86% (d6-ACAC). The larger deviation from the experiment in the d6-ACAC ν_{OH} frequency may be due to the inclusion of only two Fermi resonance interactions (see Refs. [21] and [27]), with $\nu_7 + \nu_{22}$ and $\nu_9 + \nu_{11}$. In contrast, the OH-stretch band has a bandwidth of few hundred cm^{-1}, and the experimental assignment of 2761 cm^{-1} is only approximative. Also, Tables I–IV present harmonic IR intensities. The value of a harmonic intensities are comperable to the experimental ones, with a larger discrepancy seen only in the case of a ν_{OH} d6-ACAC fundamental again.

TABLE IV

B1LYP/6-311G(*d,p*) vibrational frequencies cm^{-1} of TS2-ACAC conformer.

	B1LYP(h)	Int.	B1LYP(a)	Mode
1	3225	1	3098	ν $CH_{olefinic}$
2	3148	4	2997	ν_a CH_3
3	3137	7	2987	ν_a CH_3
4	3112	2	2984	ν_a CH_3
5	3101	2	2961	ν_a CH_3
6	3091	90	2487	ν OH
7	3051	1	2951	ν_s CH_3
8	3048	1	2943	ν_s CH_3
9	1691	100	1644	ν_a C═C─C═O + δ OH
10	1656	80	1628	ν C═O + δ OH
11	1506	15	1466	δ_a CH_3
12	1492	1	1447	δ_a CH_3
13	1482	3	1443	δ_a CH_3
14	1479	2	1438	δ_a CH_3
15	1470	44	1437	ν_a C─C═C─O + δ CH + δ OH + ν C─CH_3
16	1421	5	1380	δ_s CH_3 + δ OH
17	1402	9	1371	δ_s CH_3 + δ OH
18	1393	37	1318	δ OH + ν C═O + ν_s C─C═C─O
19	1273	43	1242	ν_s C─C═C + δ OH + ν C─CH_3
20	1199	7	1178	δ $CH_{olefinic}$
21	1073	1	1048	π CH_3
22	1053	5	1031	π CH_3
23	1040	2	1022	ρ CH_3
24	1026	3	1008	ρ CH_3
25	987	22	965	γ OH
26	953	2	939	δ C─C═C + ν C─C + ρ CH_3
27	933	4	916	ν C─CH_3 + ν C─O
28	799	9	758	γ $CH_{olefinic}$
29	665	—	657	Γ_{ring}
30	641	4	635	Δ_{ring}
31	562	—	561	Γ_{ring}
32	510	4	511	Δ_{ring}
33	406	1	405	Δ_{ring}
34	373	2	363	ν O$\cdots$O
35	235	1	224	Γ_{ring} + γ C─CH_3
36	182	—	176	Γ_{ring} + τ CH_3
37	153	—	146	τ CH_3
38	122	—	106	τ CH_3
39	54.492*i*	—	32.501*i*	τ CH_3

A nonperturbative description of the ν_{OH} band requires knowledge of the multidimensional potential energy surface (PES). This topic is beyond scope of the present study. However, two-dimensional cuts of the PES already provide insight into the mode-mixing dynamics. Besides the low-frequency modes modifying the inter-oxygen distance, the OH-stretching vibration appears to be strongly coupled to the CH_3 torsion modes. To gain a better understanding of these effects, we have calculated the anharmonic vibrational frequencies of the **TS2** rotamer (see Fig. 1). The results are given in Table IV. In **TS2**, the OH-stretch fundamental is located at 2487 cm^{-1}. Compared with the anharmonic frequency of the **SYN** structure, the mode is red-shifted by 280 cm^{-1}. This large difference suggests that the extreme broadness of the ν_{OH} band in the IR spectrum of ACAC may be caused by the coexistence of the **SYN** and **TS2** structures the gas phase.

Next we focus on the 1000–1700 cm^{-1} region, where the harmonic analysis predicts five modes made up from OH in-plane bending and C═O,

C—O, C=C, and C—C stretching. Two transitions are observed in the deconvoluted spectrum of ACAC in the C=O stretch region: a superposition of the asymmetric C=C—C=O stretch with the OH in-plane bending at 1642 cm^{-1} and the C=O stretching coupled to OH in-plane bending at 1624 cm^{-1}. At low temperature, however, the C=O band splits into three components [16], while two components can be seen in the d2-ACAC spectrum at all temperatures. These features have been attributed by Cohen and Weiss [16] to the fast interconversion of two energetically close forms of ACAC, presumably to **TS2** and **SYN**. The harmonic analysis of Ref. [15] confirmed this assignment. In this frequency range, we located two normal modes at 1650 cm^{-1} and 1625 cm^{-1}, both in very satisfactory agreement with room temperature data. In the **TS2** rotamer, the two modes shift for only few wavenumbers to 1644 and 1628 cm^{-1}. The difference between the **SYN** and **TS2** frequencies is obviously too small to explain the three-maxima structure of the band. No other mode is close to this range, and combination transitions are expected to be much weaker. At low temperatures, contributions from the energetically less favorable **TS1** rotamer can also be disregarded. Thus, the provided pieces of information are difficult to reconcile with previous assignments, and we leave the topic open for discussion.

Finally, we address the lower-frequency OH in-plane bending mode coupled to the symmetric C=O and C—C=C—O stretch. The bending transition has not been observed in the gas phase due to the overlap with one of the keto bands. However, it has been observed in rare gas matrices at 1288 cm^{-1} [28] and after deconvolution of the liquid phase spectrum at 1302 cm^{-1}. Our calculation yielded 1345 cm^{-1} for the **SYN** conformation and 1318 cm^{-1} for the **TS2** conformation. Taking into account that transitions in rare gas matrices are shifted downward in comparison with the gas phase, we attributed the line to the **TS2** conformer.

4. Summary

A quantum mechanical study of the enolic form of ACAC at the MP2 and B1LYP levels of theory is presented. Two conformers, **SYN** and **TS2**, are separated by an energy barrier of 0.25 kcal mol^{-1} at the MP2(FC)/6-311G(*d,p*) and 0.13 kcal mol^{-1} at the B1LYP/6-311G(*d,p*) level of theory. Their contribution to the vibrational spectrum is analyzed and the signature of both conformers is found in the spectrum. Specifically, the large difference in the OH-stretch frequencies between the **SYN** and **TS2** conformers finds agreement with the broadness of the experimental band. The frequency shift of the ν_{17} (OH-bend/symmetric C=O, C—C=C—O stretch) fundamental can also be attributed to **TS2**. In contrast, the fast interconversion between the two forms cannot explain the three-maxima shape of the C=O stretch band. On this issue, future investigation should go beyond the normal-mode analysis and should take into account the large-amplitude motion of the transferring proton [29].

ACKNOWLEDGMENTS

The authors are grateful to V. Mohaček-Grošev (RBI, Zagreb) for stimulating discussions. This work has been supported by the Croatian Ministry of Science and Technology under project 0098033, and by the Humboldt Foundation (to N.D.).

References

1. Hadži, D. Theoretical Treatments of Hydrogen Bonding; John Wiley & Sons: Chichester, UK, 1997.
2. Emsley, J. Struct Bond 1984, 57, 147.
3. Bratos, S.; Leicknam, J.; Gallot, G.; Ratajczak, H. In Ultrafast Hydrogen Bonding Dynamics and Proton Transfer Processes in the Condensed Phase; Elsaesser, T.; Bakker, H., Eds.; Kluwer Academic: Dordrecht, the Netherlands, 2002; p 5.
4. Chamma, D.; Valcescu, A.; Blaise, P.; Henri-Rousseau, O. Chem Phys 2003, 293, 23.
5. Belharaya, K.; Blaise, P.; Henri-Rousseau, O. Chem Phys 2003, 293, 9.
6. Došlić, N.; Kühn, O. Z Phys Chem 2003, 217, 1507.
7. Heyne, K.; Huse, N.; Nibbering, E.; Elsaesser, T. Chem Phys Lett 2003, 369, 591.
8. Heyne, K.; Huse, N.; Nibbering, E.; Elsaesser, T. Chem Phys Lett 2003, 382, 19.
9. Smith, Z.; Wilson, E. B.; Duerst, R. W. Spectrochim Acta A 1983, 39, 1117.
10. Chiavassa, T.; Roubin, P.; Pizzala, L.; Verlaque, P.; Allouche, A.; Marinalli, F. J Phys Chem 1992, 96, 10659.
11. Ogoshi, H.; Nakamoto, K. J Chem Phys 1966, 45, 3113.
12. Tayyari, S. F.; Zeegers-Huyskens, T.; Wood, J. L. Spectrochim Acta A 1979, 35, 1289.
13. Mavri, J.; Grdadolnik, J. J Phys Chem A 2001, 105, 2045.
14. Mavri, J.; Grdadolnik, J. J Phys Chem A 2001, 105, 2039.
15. Tayyari, S. F.; Milani-nejad, F. Spectrochim Acta A 2000, 56, 2679.
16. Cohen, B.; Weiss, S. J Phys Chem 1984, 88, 3159.
17. Adamo, C.; Barone, V. Chem Phys Lett 1997, 274, 242.
18. Frisch, M. J.; Trucks, G. W.; Schlegel, H. B.; Scuseria, G. E.; Robb, M. A.; Cheeseman, J. R.; Montgomery, Jr, J. A.; Vreven, T.;

Kudin, K. N.; Burant, J. C.; Millam, J. M.; Iyengar, S. S.; Tomasi, J.; Barone, V.; Mennucci, B.; Cossi, M.; Scalmani, G.; Rega, N.; Petersson, G. A.; Nakatsuji, H.; Hada, M.; Ehara, M.; Toyota, K.; Fukuda, R.; Hasegawa, J.; Ishida, M.; Nakajima, T.; Honda, Y.; Kitao, O.; Nakai, H.; Klene, M.; Li, X.; Knox, J. E.; Hratchian, H. P.; Cross, J. B.; Adamo, C.; Jaramillo, J.; Gomperts, R.; Stratmann, R. E.; Yazyev, O.; Austin, A. J.; Cammi, R.; Pomelli, C.; Ochterski, J. W.; Ayala, P. Y.; Morokuma, K.; Voth, G. A.; Salvador, P.; Dannenberg, J. J.; Zakrzewski, V. G.; Dapprich, S.; Daniels, A. D.; Strain, M. C.; Farkas, O.; Malick, D. K.; Rabuck, A. D.; Raghavachari, K.; Foresman, J. B.; Ortiz, J. V.; Cui, Q.; Baboul, A. G.; Clifford, S.; Cioslowski, J.; Stefanov, B. B.; Liu, G.; Liashenko, A.; Piskorz, P.; Komaromi, I.; Martin, R. L.; Fox, D. J.; Keith, T.; Al-Laham, M. A.; Peng, C. Y.; Nanayakkara, A.; Challacombe, M.; Gill, P. M. W.; Johnson, B.; Chen, W.; Wong, M. W.; Gonzalez, C.; Pople, J. A. Gaussian 03; Revision B.05; Gaussian: Pittsburgh, PA, 2003.

19. Schmidt, M. W.; Baldridge, K. K.; Boatz, J. A.; Elbert, S. T.; Gordon, M. S.; Jensen, J. H.; Koseki, S.; Matsunaga, N.; Nguyen, K. A.; Su, S.; Windus, T. L. J Comput Chem 1993, 14, 1347.
20. Barone, V.; Manichino, C. J Mol Struct 1995, 330, 365.
21. Barone, V.; J Chem Phys 2005, 122, 014108.
22. Folkendt, M.; Weiss-Lopez, B.; Chauvrel, J.; True, N. S. J Phys Chem 1985, 89, 3347.
23. Sliznev, V.; Lapshina, S.; Girichev, G. J Struct Chem 2002, 43, 47.
24. Matanović, I.; Došlić, N.; Mihalić, Z. Chem Phys 2004, 306, 201.
25. Johnson, M.; Jones, N.; Geis, A.; Horsewill, A.; Trommsdorff, H. P. J Chem Phys 2002, 116, 5694.
26. Frisch, M. J.; Trucks, G. W.; Schlegel, H. B.; Scuseria, G. E.; Robb, M. A.; Cheeseman, J. R.; Zakrzewski, V. G.; Montgomery, Jr, J. A.; Stratmann, R. E.; Burant, J. C.; Dapprich, S.; Millam, J. M.; Daniels, A. D.; Kudin, K. N.; Strain, M. C.; Farkas, O.; Tomasi, J.; Barone, V.; Cossi, M.; Cammi, R.; Mennucci, B.; Pomelli, C.; Adamo, C.; Clifford, S.; Ochterski, J.; Petersson, G. A.; Ayala, P. Y.; Cui, Q.; Morokuma, K.; Malick, D. K.; Rabuck, A. D.; Raghavachari, K.; Foresman, J. B.; Cioslowski, J.; Ortiz, J. V.; Stefanov, B. B.; Liu, G.; Liashenko, A.; Piskorz, P.; Komaromi, I.; Gomperts, R.; Martin, R. L.; Fox, D. J.; Keith, T.; Al-Laham, M. A.; Peng, C. Y.; Nanayakkara, A.; Gonzalez, C.; Challacombe, M.; Gill, P. M. W.; Johnson, B.; Chen, W.; Wong, M. W.; Andres, J. L.; Gonzalez, C.; Head-Gordon, M.; Replogle, E. S.; Pople, J. A. Gaussian 98; Revision A.11; Gaussian: Pittsburgh, PA, 2001.
27. Martin, J. M. L.; Lee, T. J.; Taylor, P. R.; Francois, J. J Chem Phys 1995, 103, 2589.
28. Chiavassa, T.; Verlaque, P.; Pizzala, L.; Roubin, P. Spectrochim Acta A 1994, 50, 343.
29. Matanović, I.; Došlić, N. J Phys Chem 2005, 109, 4185.